

# AR-A014418 regulates intronic polyadenylation and transcription of PD-L1 through inhibiting CDK12 and CDK13 in tumor cells

Ganggang Zhang <sup>1</sup>, Bin Lan,<sup>2</sup> Xin Zhang,<sup>1</sup> Mengyao Lin,<sup>1</sup> Yi Liu,<sup>3</sup> Junsong Chen,<sup>1</sup> Fang Guo<sup>1</sup>

**To cite:** Zhang G, Lan B, Zhang X, *et al.* AR-A014418 regulates intronic polyadenylation and transcription of PD-L1 through inhibiting CDK12 and CDK13 in tumor cells. *Journal for ImmunoTherapy of Cancer* 2023;11:e006483. doi:10.1136/jitc-2022-006483

► Additional supplemental material is published online only. To view, please visit the journal online (<http://dx.doi.org/10.1136/jitc-2022-006483>).

GZ and BL contributed equally.

Accepted 30 March 2023



© Author(s) (or their employer(s)) 2023. Re-use permitted under CC BY-NC. No commercial re-use. See rights and permissions. Published by BMJ.

<sup>1</sup>Key Laboratory of Systems Biomedicine (Ministry of Education), Shanghai Center for Systems Biomedicine, Shanghai Jiao Tong University, Shanghai, China

<sup>2</sup>Fujian Provincial Key Laboratory of Tumor Biotherapy, Clinical Oncology School of Fujian Medical University, Fujian Cancer Hospital, Fuzhou, Fujian, China

<sup>3</sup>Department of Radiation Oncology, Zhongshan Hospital, Fudan University, Shanghai, China

## Correspondence to

Dr Fang Guo; [fguo@sjtu.edu.cn](mailto:fguo@sjtu.edu.cn)

## ABSTRACT

**Background** Immune checkpoint molecules, especially programmed death 1 (PD-1) and its ligand, programmed death ligand 1 (PD-L1), protect tumor cells from T cell-mediated killing. Immune checkpoint inhibitors, designed to restore the antitumor immunosurveillance, have exhibited significant clinical benefits for patients with certain cancer types. Nevertheless, the relatively low response rate and acquisition of resistance greatly limit their clinical applications. A deeper understanding of the regulatory mechanisms of PD-L1 protein expression and activity will help to develop more effective therapeutic strategies.

**Methods** The effects of AR-A014418 and THZ531 on PD-L1 expression were detected by western blot, reverse transcription-quantitative polymerase chain reaction (RT-qPCR) and flow cytometry. In vitro kinase assays with recombinant proteins were performed to confirm that AR-A014418 functioned as a CDK12 and CDK13 dual inhibitor. The roles of CDK12 and CDK13 in intronic polyadenylation (IPA) and transcription of PD-L1 were determined via RNA interference or protein overexpression. T-cell cytotoxicity assays were used to validate the activation of antitumor immunity by AR-A014418 and THZ531.

**Results** AR-A014418 inhibits CDK12 to enhance the IPA, and inhibits CDK13 to repress the transcription of PD-L1. IPA generates a secreted PD-L1 isoform (PD-L1-v4). The extent of IPA was not enough to reduce full-length PD-L1 expression obviously. Only the superposition of enhancing IPA and repressing transcription (dual inhibition of CDK12 and CDK13) dramatically suppresses full-length PD-L1 induction by interferon- $\gamma$ . AR-A014418 and THZ531 could potentiate T-cell cytotoxicity against tumor cells.

**Conclusions** Our work identifies a new regulatory pathway for PD-L1 expression and discovers CDK12 and CDK13 as promising drug targets for immune modulation and combined therapeutic strategies.

## INTRODUCTION

Currently ongoing clinical trials and approved drugs for cancer immunotherapy are mainly focused on monoclonal antibodies blocking the programmed death 1 (PD-1)/programmed death ligand 1 (PD-L1) axis. PD-L1 (also known as CD274 or B7H1)

## WHAT IS ALREADY KNOWN ON THIS TOPIC

⇒ The interaction between full-length PD-L1 on tumor cells and its receptor PD-1 on T cells attenuates T cell activation and cytotoxicity against tumor cells. Reducing full-length PD-L1 levels, either genetically or pharmacologically, would reactivate antitumor T-cell immunity.

## WHAT THIS STUDY ADDS

⇒ CDK12 and CDK13 regulates the intronic polyadenylation and transcription of PD-L1. AR-A014418 also functions as a CDK12/CDK13 inhibitor. Both AR-A014418 and CDK12/CDK13 dual inhibitor, THZ531, suppress full-length PD-L1 induction by IFN- $\gamma$ , thus potentiate T-cell cytotoxicity against tumor cells.

## HOW THIS STUDY MIGHT AFFECT RESEARCH, PRACTICE OR POLICY

⇒ Our work indicates that CDK12/CDK13 are probably meaningful targets for developing small-molecule immune checkpoint inhibitors.

is expressed on the plasma membrane of tumor cells and stromal cells. The binding of PD-L1 to its receptor PD-1, which is expressed on cytotoxic T lymphocytes (CTLs), inhibits T-cell proliferation, cytokine production, and cytotoxicity to tumor cells.<sup>1</sup> Antibody drugs targeting PD-L1 or PD-1 could efficiently block the extracellular ligation to restore T-cell function, and have been successfully translated into clinical applications, treating melanoma, non-small cell lung cancer, renal cell carcinoma, and several other cancers. However, even though some patients achieve durable tumor remission, more patients do not respond to or quickly become resistant to immune checkpoint blockade.<sup>2</sup> To develop more effective drugs and combination strategies, it is necessary to understand the molecular regulation of PD-L1 expression and activity in tumor cells.

Regulation of PD-L1 at the epigenetic,<sup>3</sup> transcriptional,<sup>4</sup> post-transcriptional,<sup>5</sup> translational<sup>6</sup> and post-translational<sup>7–9</sup> levels have been widely investigated. The establishment of PD-L1 regulatory networks provides numerous opportunities for developing small-molecule drugs to reactivate antitumor immunity by manipulating PD-L1 expression.<sup>8–10</sup> However, chemotherapies or targeted agents may cause tumor immunoevasion by upregulating PD-L1, the combination with PD-L1 or PD-1 blockade would bring more clinical benefits.<sup>11–12</sup>

PD-L1 is a type I transmembrane protein containing an extracellular immunoglobulin V-like domain (IgV, PD-1 binding region), an IgC domain, a transmembrane domain and a short cytoplasmic tail.<sup>13–14</sup> There are four transcript variants of PD-L1 annotated in the RefSeq database (<https://www.ncbi.nlm.nih.gov/refseq/>). Variant 1 (NM\_014143.4) encodes the well-researched full-length PD-L1. Variant 2 (NM\_001267706.2) and variant 3 (NR\_052005.2), generated through alternative splicing, produce an isoform missing the PD-1 binding domain<sup>15</sup> or a non-coding transcript,<sup>16</sup> respectively. Recognition of an alternative polyadenylation signal (PAS, still not definitively identified) located within the fourth intron leads to premature transcriptional termination. The resulting variant 4 (NM\_001314029.2) includes the first four exons and part of the fourth intron, thus encodes a secreted isoform (PD-L1-v4).<sup>17–18</sup> PD-L1-v4 is widely expressed in multiple cancers and normal tissues. As a newly identified isoform, its role in cancer immunology is still controversial. The biogenesis and exact activity of PD-L1-v4 deserve further investigation.

The 3' end formation of RNA polymerase II (Pol II)-derived transcripts can be divided into two consecutive steps: endonucleolytic cleavage at the polyadenylation sites (PA-site) and addition of poly(A) tails. Over 70% of human genes harbor multiple PA-sites that can be alternately used for polyadenylation to generate RNAs with different 3' ends.<sup>19</sup> Most PA-sites locate within the 3'-untranslational region (3' UTR) to control messenger RNA (mRNA) stability, localization and translation. But when PA-sites in the internal introns or exons are used, alternative polyadenylation results in truncated proteins exhibiting diminished or changed function.<sup>20</sup> Cyclin-dependent kinase 12 and 13 (CDK12 and CDK13) are evolutionarily related serine-threonine kinases, with similar catalytic domain and sharing a regulatory cyclin, cyclin K.<sup>21</sup> The two kinases exhibited both redundant and distinct roles in controlling transcription elongation, mRNA splicing and 3' end processing by phosphorylating RNA processing factors and C-terminal domain (CTD) of Pol II.<sup>22–24</sup> Genetic depletion or pharmacological inhibition of CDK12 has long been discovered to abrogate the expression of multiple DNA damage response (DDR) genes, leading to defective homologous recombination repair.<sup>21–25–26</sup> Until recently, it was confirmed that CDK12 suppresses intronic polyadenylation (IPA) of transcripts containing multiple intronic PA-sites, especially DDRs, enabling the production of functional full-length

proteins.<sup>24–27</sup> Dual inhibition of CDK12 and CDK13 was shown to trigger extensive genome-wide transcriptional changes including widespread IPA.<sup>28</sup> However, the underpinning molecular mechanisms by which CDK12 and CDK13 regulate IPA remain poorly understood.

AR-A014418 has long been considered as a highly selective GSK3 $\alpha$ / $\beta$  inhibitor.<sup>29</sup> Here, we found that AR-A014418 decreased interferon (IFN)- $\gamma$  induced full-length PD-L1 expression in multiple cancer cells via inhibiting CDK12 and CDK13 rather than GSK3 $\alpha$ / $\beta$ . CDK12 limits the IPA at intron 4, and CDK13 regulates PD-L1 transcription. The superposition of enhancing IPA and repressing transcription leads to reduced full-length PD-L1 induction. Therefore, pharmacologically inhibiting CDK12/CDK13 represents a meaningful strategy to rebuild the host immune surveillance.

## METHODS

### Cell lines

All cell lines used in this study were obtained from the American Type Culture Collection. A375, HeLa, SW1990, MDA-MB-231, HCT116, M21, B16F10, Rm-1, MC38 cells were cultured in Dulbecco's Modified Eagle's Medium (DMEM) supplemented with 10% fetal bovine serum (FBS), 50  $\mu$ g/mL penicillin and 50 mg/mL streptomycin (Gibco). BxPC3, THP-1, CT26 cells were grown in Roswell Park Memorial Institute (RPMI) 1640 medium supplemented with FBS and penicillin/streptomycin.

### Western blot assays

Cells were lysed directly in 1 $\times$ loading buffer (50 mM Tris pH6.8, 2% SDS, 10% glycerol, 100 mM DTT, 0.01% bromophenol blue). Protein samples were resolved on 8% or 10% SDS-PAGEs and transferred to 0.45  $\mu$ m PVDF membranes (Merck Millipore). Image acquisition was performed using an Amersham Imager 600 (GE Healthcare).

### Flow cytometry analysis

Cells were collected by trypsin digestion and blocked with 3% bovine serum albumin (BSA). Human cancer cells were incubated with mouse anti-hPD-L1 antibody (329702, BioLegend) for 30 min. After washing three times with 1% BSA, the cells were stained with PE-conjugated anti-mouse IgG secondary antibody (405307, BioLegend) for 30 min. Mouse cancer cells were stained with PE-conjugated anti-mPD-L1 antibody (12-5982-81, Thermo Fisher) for 30 min. All operations were performed on ice. After washing three times, the stained cells were resuspended in phosphate-buffered saline (PBS) and analyzed using an LSRFortessa flow cytometer (BD Biosciences). Data was analyzed with FlowJo software.

### RT-qPCR assays

Total RNA was extracted using RNA Isolation Kit (B610583, Sangon) and subjected to ReverTra Ace qPCR RT Master Mix with gDNA Remover (FSQ-301,

TOYOBO) for complementary DNA synthesis according to the manufacturer's instructions. Genomic DNA or transfected plasmids were digested. Quantitative polymerase chain reaction (qPCR) was performed with SYBR Green Realtime PCR Master Mix (QPK-201, TOYOBO) on LightCycler 96 (Roche).  $2^{-\Delta\Delta C_t}$  method was used for data analysis. The expression of each target gene was normalized to GAPDH.

### Generation of knockout or overexpression stable cell lines

To generate GSK3 $\alpha/\beta$  or PD-L1 knockout cancer cell lines, the respective target sequences were cloned into lentiCRISPRv2 vector. Cells were transiently transfected with the recombinant plasmids using Lipo6000 Transfection Reagent (C0526, Beyotime), followed by puromycin (A610593, Sangon) selection. Survived cells were plated in limiting dilution in 96-well plates to isolate single-cell colonies. Knockout of the target genes was confirmed by western blot.

To establish stable cell lines overexpressing PD-L1-v1/v4, CDK13 or RPL22-3 $\times$ HA, the coding sequences were cloned into pCDH-CMV-MCS-EF1-Puro vector (CD510B-1, System Biosciences). Packaging of lentivirus was carried out in 293T cells by co-transfecting the recombinant plasmids and virus packaging vectors (pMD2.G and psPAX2). Virus-containing medium was concentrated using 3 $\times$ PEG collection medium. Cells were infected with virus in the presence of 10  $\mu$ g/mL polybrene and screened by puromycin.

### Transfection of siRNAs

Small interfering RNAs (siRNAs) targeting human CDK12 or CDK13 were transfected into A375 and Hela cells using Lipo6000 at a final concentration of 60 nM. IFN- $\gamma$  was added 30 hours after transfection and the cells were collected for reverse transcription-quantitative polymerase chain reaction (RT-qPCR) (12 hours after IFN- $\gamma$ ) or western blot (16 hours after IFN- $\gamma$ ) at the indicated time.

### Analysis of PD-L1 protein stability

Cancer cells were treated with IFN- $\gamma$  (100  $\mu$ g/mL) for 24 hours to induce PD-L1 expression. Medium was then changed to normal complete DMEM and cycloheximide (CHX, 100  $\mu$ g/mL) was added to inhibit protein synthesis together with or without AR-A014418. PD-L1 protein levels were determined at the indicated time points through western blot and were normalized to GAPDH.

### Stability of PD-L1 mRNA variants

For PD-L1 mRNA stability studies, A375 cells were treated with IFN- $\gamma$  (100  $\mu$ g/mL) for 10 hours to induce PD-L1 expression. Then, DMSO or AR-A014418 was added to the culture medium. Actinomycin D (10  $\mu$ g/mL) was added to stop mRNA transcription 1 hour later. Total RNA was isolated at 0, 1, 2 and 4 hours to measure levels of PD-L1 v1 and v4 by RT-qPCR. The data was normalized to GAPDH mRNA.

### PD-L1 and PD-1 binding assay

To measure PD-L1 and PD-1 protein interaction, cells were detached with trypsin-digestion, incubated with 5  $\mu$ g/mL recombinant human PD-1 FC chimera protein (1086-PD-050, R&D) at room temperature for 30 min, washed two times and further stained with PE conjugated Goat anti-Human IgG Fc secondary antibody (12-4998-82, Thermo Fisher) for 30 min. The stained cells were washed and resuspended in PBS. Data was collected using LSR Fortessa flow cytometer and analyzed by FlowJo software.

### T-cell cytotoxicity assay

To acquire activated T cells, peripheral blood mononuclear cells (70025, STEMCELL Technologies) were cultured in complete RPMI 1640 medium supplemented with ImmunoCult Human CD3/CD28 T Cell Activator (10991, STEMCELL Technologies) for 5–7 days. Cancer cells were allowed to adhere to the plates overnight and co-cultured with activated T cells (MDA-MB-231-to-T cell ratio, 1:2) for 48 hours in the presence or absence of AR-A014418 or THZ531. T cells and cell debris were removed by washing with PBS (three times), living cancer cells were stained with crystal violet, washed four times with ddH<sub>2</sub>O. The plates were photographed. The crystal violet was resolved from cells by 33% acetic acid and then quantified at OD 570 nm using a spectrometer to calculate the survival rates.

### Statistical analysis

Numerical data were presented as mean $\pm$ SD fold change relative to control groups of three independent experiments. All data analyses were performed in GraphPad Prism (V.9) using the unpaired, two-tailed t-test module. A p value < 0.05 was considered statistically significant.

## RESULTS

### AR-A014418 suppresses IFN- $\gamma$ induced full-length PD-L1 expression via unknown targets but not GSK3 $\alpha/\beta$

GSK3 $\alpha/\beta$  are constitutively active serine/threonine kinases with a wide substrate spectrum, thus performing critical functions in many cellular processes, including glycogen metabolism, transcription, translation and protein degradation.<sup>30</sup> Both GSK3 $\alpha$  and GSK3 $\beta$  were shown to directly phosphorylate PD-L1 to promote its proteasomal degradation.<sup>7,9</sup> Activation of GSK3 $\alpha/\beta$  by EGFR inhibitors destabilized PD-L1, enhanced T cell-mediated cytotoxicity and improved efficacy of checkpoint blockade therapies.<sup>7,9</sup> Inactivation of GSK3 $\alpha/\beta$  by MET or PARP inhibitors produced the opposite effects by stabilizing PD-L1.<sup>11,12</sup> These studies imply a negative correlation between GSK3 $\alpha/\beta$  kinase activity and PD-L1 protein level.

The inflammatory cytokine IFN- $\gamma$ , secreted by CTLs, is the best-characterized stimulus for PD-L1 within the tumor microenvironment.<sup>31</sup> Interestingly, we found that AR-A014418 significantly decreased the total protein level and cell surface expression of full-length PD-L1 induced



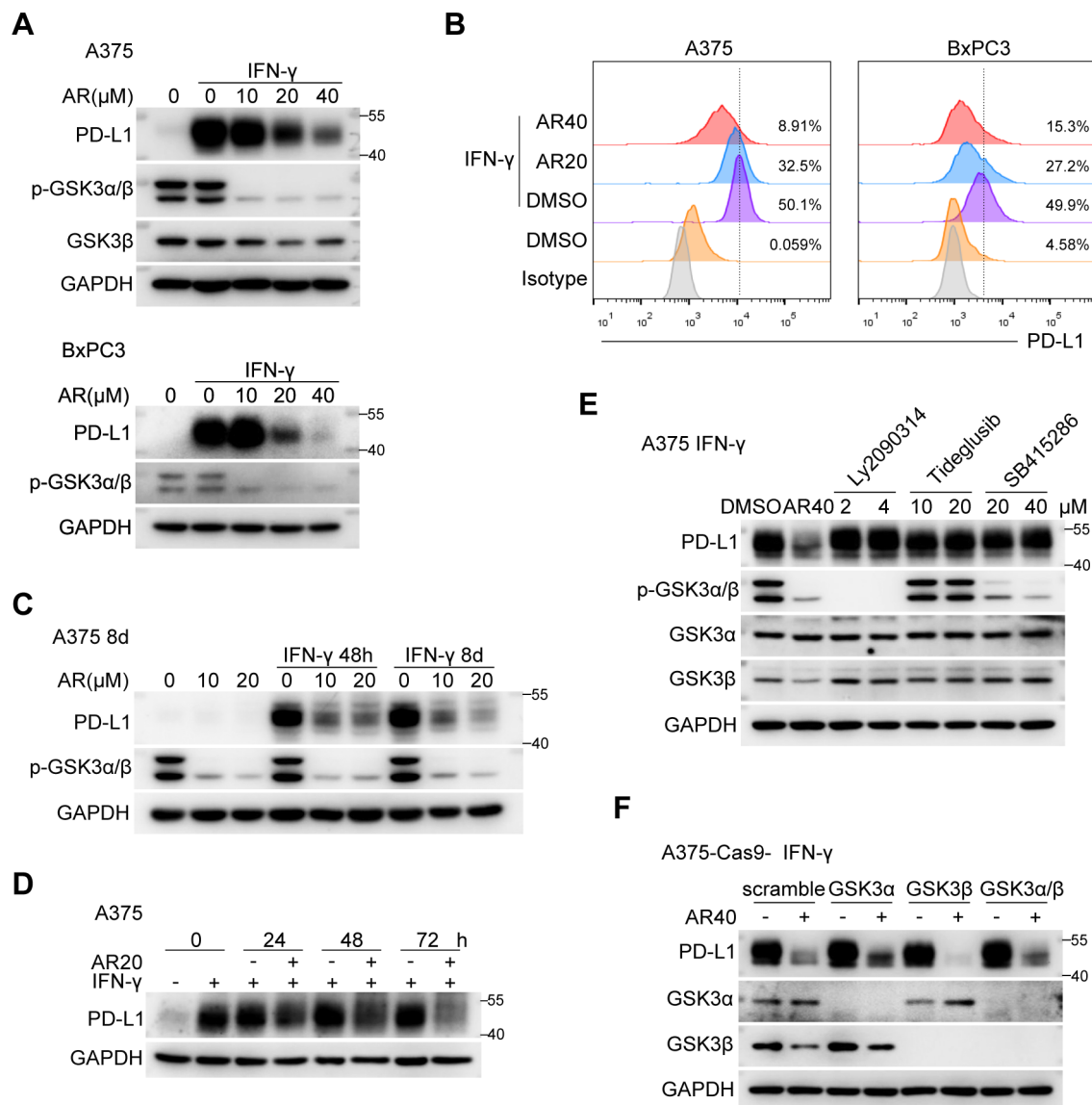


**Figure 1** AR-A014418 suppresses full-length PD-L1 expression induced by IFN- $\gamma$  through unknown targets. (A) A375 and BxPC3 cells were treated with IFN- $\gamma$  (100 ng/mL) and the indicated concentrations of AR-A014418 for 24 hours, the whole-cell lysates were subjected to western blot analysis. (B) Flow cytometry analysis of cell surface PD-L1 level in A375 and BxPC3 cells treated with IFN- $\gamma$  and AR-A014418 for 24 hours. (C) A375 cells were cultured with AR-A014418 at indicated concentrations for 8 days, IFN- $\gamma$  treatment was carried out at the beginning (8 days) or the last 48 hours (48 hours). (D) A375 cells were preincubated with IFN- $\gamma$  for more than 3 days. DMSO/AR-A014418 (20  $\mu$ M) were added to the culture medium in the presence of IFN- $\gamma$  at 0 hour. Samples were collected at 24, 48 and 72 hours. (E) A375 cells were treated with AR-A014418, Ly2090314, Tideglusib or SB415286 together with IFN- $\gamma$  for 24 hours and analyzed by western blot. (F) Western blot analysis of full-length PD-L1 induction in control or GSK3 $\alpha$  and/or GSK3 $\beta$  knockout A375 cells. IFN, interferon; PD-L1, programmed death ligand 1.

by IFN- $\gamma$  in multiple tumor cell lines (figure 1A,B; online supplemental figure S1A-C). But basal PD-L1 protein level was not altered or was slightly increased (online supplemental figure S1D,F). The inhibitory effect of AR-A014418 on PD-L1 induction is universal and lasting, because it is consistent in all cell lines we examined whose PD-L1 could be upregulated by IFN- $\gamma$  and it still works after long-term drug treatment (figure 1C). In tumor cells preincubated with IFN- $\gamma$ , AR-A014418 was also able to reduce the expression of 'steady-state' PD-L1 (figure 1D). We therefore considered AR-A014418 as a potential immunotherapeutic agent.

Phosphorylation at Y279-GSK3 $\alpha$  or Y216-GSK3 $\beta$  is required for the full kinase activity.<sup>32</sup> 10  $\mu$ M AR-A014418 was enough to inhibit phosphorylation at these sites (figure 1A). It is puzzling that suppression of PD-L1 induction by AR-A014418 contradicts the known consequences of GSK $\alpha$ / $\beta$  inactivation. To validate whether the suppressive effect was achieved through interfering with GSK3 $\alpha$ / $\beta$  signaling, A375 and B16F10 cells were treated with other GSK3 inhibitors. As shown in figure 1E and online supplemental figure S2A, Ly2090314, Tideglusib and SB415286 did not block full-length PD-L1 induction as AR-A014418. Depletion of GSK3 $\alpha$  and/or GSK3 $\beta$

also had no effect on PD-L1 expression and inhibition (figure 1F). Consistent with the knockout results, over-expressing GSK3 $\alpha$  or GSK3 $\beta$  was not able to attenuate PD-L1 downregulation by AR-A014418 (online supplemental figure S2B). We thus concluded that AR-A014418 suppressed full-length PD-L1 induction by IFN- $\gamma$  via unknown targets but not GSK3 $\alpha$ / $\beta$ .

Expression of cyclin D1 and survivin or phosphorylation of 4E-BP1 at T37/46, S65, and T70 were also down-regulated by AR-A014418 (online supplemental figure S2C) as previously reported.<sup>33 34</sup> STAT1 $\alpha$  has been well documented as a positive regulator for PD-L1 induction by IFN- $\gamma$ , largely through activating its transcription.<sup>35–37</sup> Stimulation with IFN- $\gamma$  led to a strong increase of STAT1 $\alpha$  expression, which can be repressed by AR-A014418 (online supplemental figure S2C). Unexpectedly, treatment with other GSK3 inhibitors or depletion of GSK3 $\alpha$  and/or GSK3 $\beta$  did not produce the same inhibitory effects as AR-A014418, which again emphasized the pivotal roles of unknown AR-A014418 targets.

Collectively, we demonstrated that although AR-A014418 was considered to be a selective GSK3 $\alpha$ / $\beta$  inhibitor, its suppressive effects on PD-L1 and STAT1 induction, cyclin D1 and survivin expression, or 4E-BP1 phosphorylation were not achieved through targeting GSK3 $\alpha$ / $\beta$ .

#### Total PD-L1 mRNA level, translation efficiency and protein stability are not decreased by AR-A014418

The levels of cellular proteins are determined by the dynamic balance between synthesis (transcription, mRNA processing, mRNA stability, translation) and degradation (protein stability). To unravel the biological processes of PD-L1 that are perturbed by AR-A014418, we first detected total PD-L1 mRNA level via RT-qPCR assays. One pair of primers was designed to recognize all possible PD-L1 transcripts annotated in the RefSeq database. PD-L1 protein was upregulated as early as 6 hours after IFN- $\gamma$  stimulation, and was already suppressed by AR-A014418 at this time (figure 2A). However, total PD-L1 transcripts were not downregulated by AR-A014418 during the experimental time course in A375 cells or only slightly decreased at 24 hours in BxPC3 cells (figure 2B). Therefore, we tentatively assumed that AR-A014418 may not act through inhibiting PD-L1 transcription or promoting mRNA degradation.

In response to IFN- $\gamma$ , STAT1 $\alpha$  upregulates the expression of transcription factor IRF1, which in turn enhances PD-L1 transcription.<sup>35</sup> Inhibiting STAT1 $\alpha$  protein expression almost completely blocked PD-L1 induction.<sup>36 37</sup> It is strange that AR-A014418 repressed STAT1 $\alpha$  expression, but total PD-L1 mRNA level was not decreased correspondingly (online supplemental figure S2C, figure 2B). In A375 cells treated with IFN- $\gamma$  and AR-A014418, IRF1 mRNA was significantly stimulated by IFN- $\gamma$ , and only decreased to a certain extent by AR-A014418 (online supplemental figure S3A). The remaining IRF1 may be enough for PD-L1 induction.

Several studies have characterized the lysosome or proteasome-mediated degradation of PD-L1.<sup>7 9 10</sup> Cell surface PD-L1 can also be cleaved by ADAM family metalloproteases to generate a secreted N-terminal fragment.<sup>38 39</sup> To investigate whether AR-A014418 was involved in the degradation or cleavage processes, we performed CHX chase assays in A375 and B16F10 cells. Full-length PD-L1 protein was relatively stable during the experimental period and AR-A014418 did not accelerate its degradation or cleavage (figure 2C; online supplemental figure S3B).

Hypophosphorylated 4E-BP1 competes with eIF4G for eIF4E binding to suppress cap-dependent translation. Since 4E-BP1 phosphorylation was repressed by AR-A014418, we asked whether it would inhibit translation of PD-L1. Plasmids encoding 4E-BP1 or 4E-BP1-4A, a mutant 4E-BP1 carrying alanine substitutions at T37, T46, S65 and T70 to mimic hypophosphorylated 4E-BP1, were transiently transfected into Hela cells. Overexpression of the 4E-BPs, especially 4E-BP1-4A, can theoretically repress cap-dependent translation initiation. However, the protein levels of full-length PD-L1, STAT1 $\alpha$  and survivin were not reduced as expected (figure 2D; online supplemental figure S3C). In addition, the downregulation of PD-L1 by AR-A014418 was not ameliorated by over-expressing wild-type (WT) eIF4E and the constitutively active form (S209D) (online supplemental figure S3D). To provide direct evidence for the impact of AR-A014418 on PD-L1 translation, we measured ribosome-associated mRNAs using the RiboTag method (figure 2E).<sup>40</sup> S6, a component of 40S ribosome subunit, was coprecipitated with RPL22-3 $\times$ HA, which confirmed the successful enrichment of intact ribosomes (online supplemental figure S3E). As shown in figure 2F and online supplemental figure S3F, the changes of ribosome-associated PD-L1 mRNAs under AR-A014418 treatment were consistent with total cellular PD-L1 mRNAs. AR-A014418 did not interfere with the PD-L1 translation process.

Altogether, we concluded that the total PD-L1 mRNA level, translation efficiency and protein stability are not decreased by AR-A014418.

#### AR-A014418 enhances IPA of PD-L1

Since total PD-L1 mRNA level was not downregulated by AR-A014418, we sought to assess the changes of each variant, respectively (figure 3A). Primer pairs, recognizing variant 1 (v1), variant 2 (v2), variant 3 (v3), variant 4 (v4), variant 1, 2 (v12), variant 1, 3, 4 (v134), and total PD-L1 mRNA (v1234) were used for RT-qPCR assays. Surprisingly, both v1, v2, and v3 were reduced by AR-A014418, whereas v4 was increased (figure 3B; online supplemental figure S4A). The reduction of v1 may explain the decreased expression of full-length PD-L1 protein. Ct values of v2 and v3 were much higher than that of v1 and v4, and were close to the detection limit (online supplemental figure S4B). Therefore, v1 and v4 are main PD-L1 transcripts in A375 and Hela cells, and v1234 or v134 levels are determined by the total amount of v1 and v4

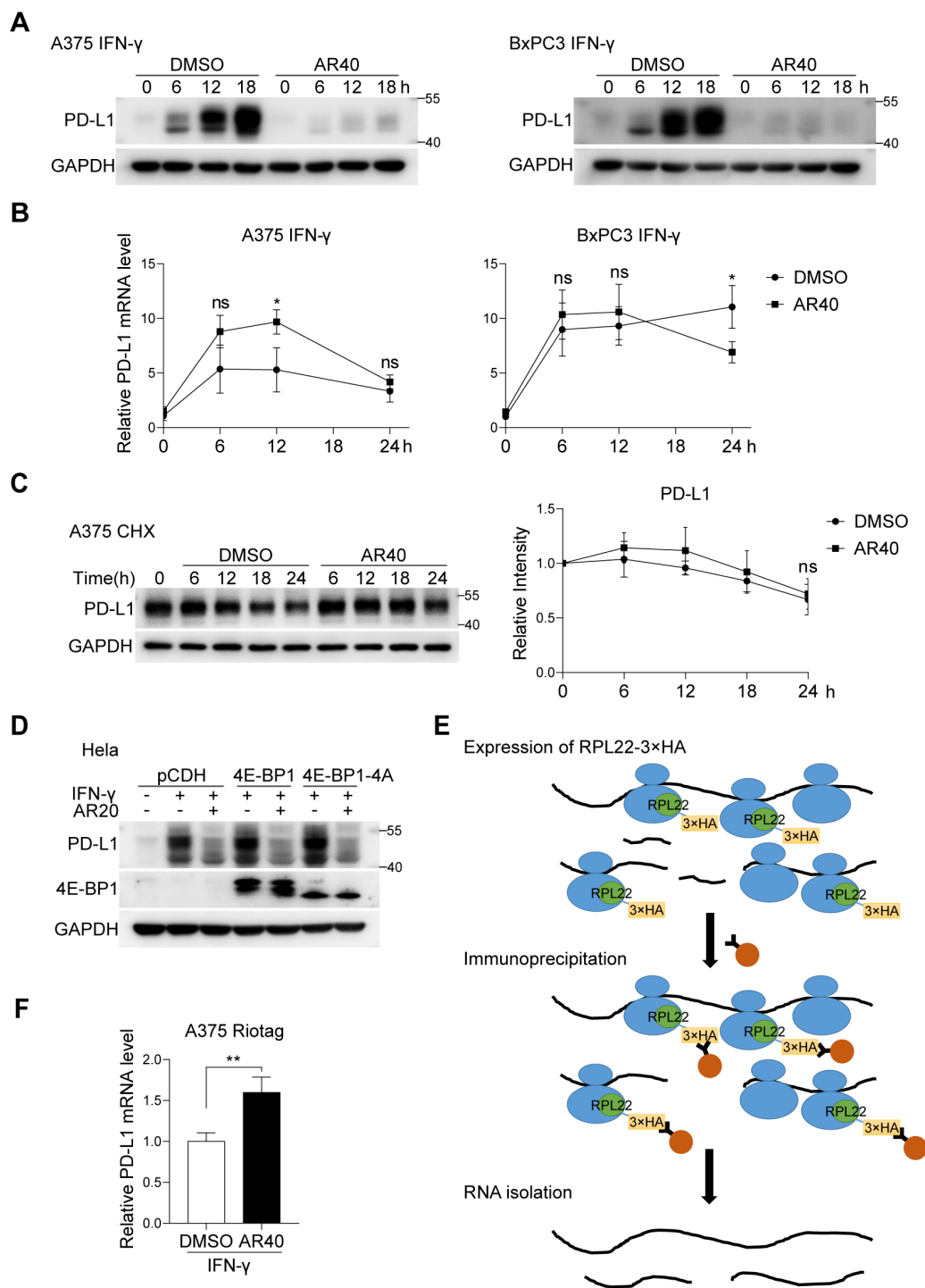


**Figure 2** AR-A014418 does not downregulate total PD-L1 mRNA level, accelerate protein degradation or prevent mRNA translation. (A) A375 and BxPC3 cells (pretreated with 40  $\mu$ M AR-A014418 for 2 hours) were stimulated by IFN- $\gamma$ , and lysed at 0, 6, 12 or 18 hours. Full-length PD-L1 expression were detected via western blot. (B) RT-qPCR analysis of total PD-L1 mRNA of A375 and BxPC3 cells (pretreated with 40  $\mu$ M AR-A014418 for 2 hours) at 0, 6, 12 and 24 hours after IFN- $\gamma$  stimulation. (C) After 24 hours incubation with IFN- $\gamma$  to induce PD-L1 expression, the culture medium was replaced with fresh medium containing DMSO/AR-A014418 (40  $\mu$ M) and cycloheximide (100  $\mu$ g/mL). Cells were harvested at 0, 6, 12, 18 and 24 hours and used for western blot analysis (shown on the left). The band intensities of PD-L1 (normalized to GAPDH) were quantified with ImageJ (shown on the right). (D) HeLa cells were transiently transfected with the indicated plasmids. IFN- $\gamma$  and AR-A014418 (20  $\mu$ M) treatment was carried out 30 hours after transfection for another 12 hours. (E) Schematic illustration of the RiboTag method in this paper. (F) RT-qPCR analysis was performed to examine the levels of ribosome-bound total PD-L1 mRNA in stable A375 cells expressing RPL22-3 $\times$ HA (A375-pCDH-RPL22-3 $\times$ HA). The process is detailed in the 'online supplemental methods' section. In B, C, and F, the values are presented as mean $\pm$ SD (n=3 independent experiments); \*p<0.05, \*\*p<0.01. IFN, interferon; mRNA, messenger RNA; PD-L1, programmed death ligand 1; RT-qPCR, reverse transcription-quantitative polymerase chain reaction.

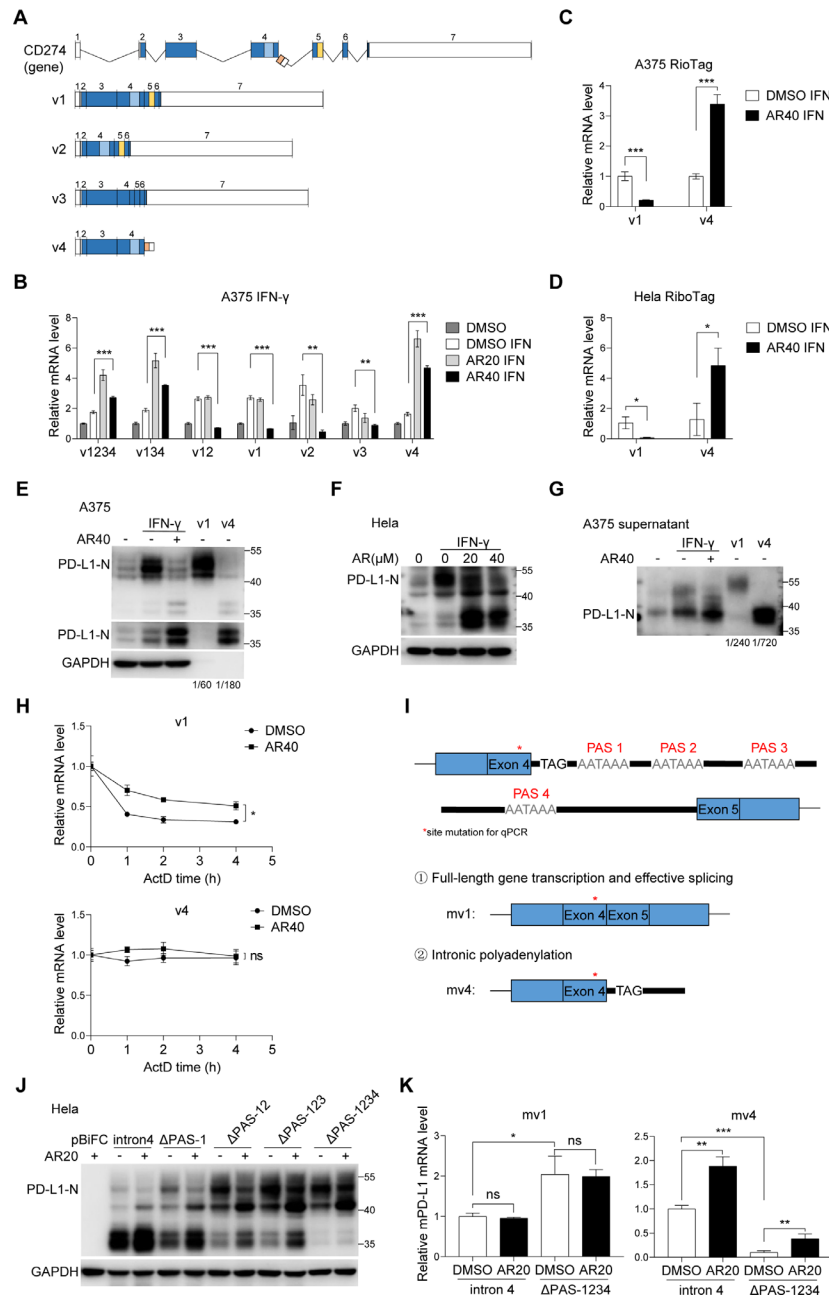


**Figure 3** The intronic polyadenylation of PD-L1 is enhanced by AR-A014418. (A) RefSeq annotated variants of PD-L1. (B) RT-qPCR analysis of indicated PD-L1 variants in A375 cells cultured with IFN- $\gamma$  and AR-A014418 (0, 20, 40  $\mu$ M) for 12 hours. (C–D) Analysis of ribosome-bound PD-L1 v1 and v4 levels in A375-pCDH-RPL22-3 $\times$ HA (C) and HeLa-pCDH-RPL22-3 $\times$ HA (D) cells by RT-qPCR. (E) A375 cells were treated with IFN- $\gamma$  and AR-A014418 for 24 hours. An antibody, which targets the N-terminal fragment of PD-L1, was applied to detect full-length PD-L1 and PD-L1-v4. Lysates of A375 stable cell lines (the right two lanes) expressing full-length PD-L1 (A375-pCDH-PD-L1-v1, 60-fold dilution) or PD-L1-v4 (A375-pCDH-PD-L1-v4, 180-fold dilution) were used to confirm the identity of the corresponding bands. (F) Western blot analysis of HeLa cells treated with IFN- $\gamma$  and AR-A014418 (0, 20, 40  $\mu$ M) for 16 hours. (G) Secreted PD-L1-v4 in the conditioned medium of indicated cells was detected using western blot. (H) DMSO or AR-A014418 (40  $\mu$ M) were added to the culture medium of A375 cells pretreated with IFN- $\gamma$  for 10 hours. An hour later, 10  $\mu$ g/mL actinomycin D (ActD) was used to stop transcription and cells were harvested at 0, 1, 2 and 4 hours post ActD addition for RT-qPCR assays. (I) Schematic illustration of the PAS deletion experiment. CTGAGT within exon 4 were mutated to TTATCG to distinguish endogenous PD-L1 transcripts without changing the amino acids. The four canonical PAS (AAUAAA), located within intron 4, were deleted sequentially. Full-length transcription and effective splicing of the minigenes would produce mutated v1 (mv1), whereas IPA would produce mutated v4 (mv4). (J–K) Minigenes were transiently transfected into HeLa cells. DMSO/AR-A014418 (20  $\mu$ M) treatment was carried out 8 hours after transfection. Cells were collected at 12 hours (for RT-qPCR, K) or 18 hours (for western blot, J) respectively, post drug treatment. In B–D, H and K, the values are presented as mean $\pm$ SD (n=3 independent experiments); \*p<0.05, \*\*p<0.01, \*\*\*p<0.001. IFN, interferon; mRNA, messenger RNA; PAS, polyadenylation signal; PD-L1, programmed death ligand 1; RT-qPCR, reverse transcription-quantitative polymerase chain reaction.



(figure 3B; online supplemental figure S4A). It is worth noting that the effects of AR-A014418 on PD-L1 mRNA expression were IFN- $\gamma$  independent, for basal PD-L1 variants changed consistently with IFN- $\gamma$  stimulated (online supplemental figure S4C,D). Basal v1 was reduced by AR-A014418, but basal full-length PD-L1 protein was not decreased or even increased (online supplemental figure S1D–F). One possible explanation is that besides downregulating v1 mRNA expression, AR-A014418 may also stabilize PD-L1 protein via inhibiting GSK3 $\alpha/\beta$ . The suppressive function of AR-A014418 on PD-L1 protein degradation is greater than on protein synthesis under normal conditions.

The changes of ribosome-associated v1 and v4 were consistent with cellular mRNA (figure 3C,D). v1 was reported to produce the full-length PD-L1 protein (40–55 kDa), but v4 produced a C-terminal truncated isoform lacking the transmembrane domain and the cytoplasmic tail (PD-L1-v4, 35–38 kDa).<sup>17 18 41</sup> A new antibody (anti-PD-L1-N) targeting the N-terminal fragment of PD-L1 was chosen to confirm the expression of full-length PD-L1 and PD-L1-v4. As shown in figure 3E,F, IFN- $\gamma$  could simultaneously stimulate the expression of both isoforms, and full-length PD-L1 was downregulated but PD-L1-v4 was upregulated by AR-A014418. Changes in PD-L1 protein expression were exactly parallel with changes in mRNA abundance. In addition, as PD-L1-v4 is a secreted isoform, it was detected in the conditioned medium of A375 cells (figure 3G). Altogether, the results indicated that AR-A014418 downregulated v1, but upregulated v4 at both mRNA and protein levels.

The 3' coding region (191 bp) and the long 3' UTR (~2700 bp) of v1 are replaced by a short 3' UTR (~60 bp) of v4 (figure 3A). In general, transcripts with longer 3' UTRs are degraded more quickly than those with shorter 3' UTRs. We thus speculated that v4 is more stable than v1. As shown in figure 3H, v1 had a short half-life, yet v4 kept stable during the trial period. Surprisingly, v1 was stabilized with AR-A014418 treatment rather than destabilized. To further clarify the impact of 3' UTR on PD-L1 mRNA stability, the coding sequence of v1 was cloned into pBiFC-VN155(I152L) vector (27097, Addgene), then the original sequence between v1 CDS and the SV40 poly(A) signal was replaced with v1 or v4 3' UTR (online supplemental figure S4E). As expected, PD-L1 mRNA level was significantly decreased by v1 3' UTR, whereas increased by v4 3' UTR (online supplemental figure S4F). AR-A014418 upregulated PD-L1 mRNA and protein expression from all three plasmids (online supplemental figure S4F,G). These results strongly supported the conclusion that v4 is more stable than v1, and AR-A014418 may play a role in stabilizing PD-L1 mRNAs.

V4 was considered to be generated by IPA due to a different 3' end from the other three variants. However, the regulatory mechanisms and biological functions of v4 are still poorly studied. In order to verify the biogenesis of v4, we constructed minigenes comprised of full-length PD-L1 CDS with an intact intron 4 between exon

4 and exon 5 (figure 3I). As shown in figure 3J, both full-length PD-L1 (from mv1) and PD-L1-v4 (from mv4) could be detected in Hela cells transiently transfected with the minigenes. Sequential deletion of the first three PAS inhibited IPA only to a certain extent, deletion of all the four canonical PAS dramatically reduced but did not completely blocked IPA, which implies that non-canonical signals may be used for compensation when the four canonical PAS are deleted (figure 3J). More importantly, AR-A014418 further elevated IPA rates of the minigenes (figure 3J,L). We asked whether AR-A014418 also controls STAT1 $\alpha$  and survivin expression via alternative polyadenylation. The 5' and 3' parts of STAT1 and survivin mRNA were decreased by AR-A014418 equally, and STAT1 $\beta$ , produced by IPA, was also reduced (online supplemental figure S4H,I). Thus, the downregulation of STAT1 $\alpha$  and survivin may be caused by transcriptional repression rather than alternative polyadenylation.

Since v4 is more stable than v1, a low ratio of IPA is able to cause high level of v4. On the other hand, v1 was slightly decreased by AR-A014418 at 20  $\mu$ M, v4 was dramatically increased (figure 3B; online supplemental figure S4D), but both v1 and v4 were reduced by AR-A014418 at 40  $\mu$ M (figure 3B; online supplemental figure S4A–D). These results led us to speculate that IPA at intron 4 alone may not be enough to significantly repress v1 expression, and AR-A014418 at high concentrations also inhibit PD-L1 transcription (initiation rate, elongation speed, or polyadenylation before intron 4).

#### AR-A014418 directly targets CDK12 and CDK13 to regulate PD-L1 expression

Transcriptional CDKs (CDK7, CDK8, CDK9, CDK11, CDK12 and CDK13) have been implicated in multiple stages of transcriptional and co-transcriptional processes.<sup>42</sup> Overexpressing CDK13, but not other CDKs, rescued the reduction of full-length PD-L1 and survivin by AR-A014418 (figure 4A; online supplemental figure S5A). CDK13 overexpression slightly increased both v1 and v4, but only v1 decrease was partially offset (figure 4B,C). Thus, we speculated that AR-A014418 inhibits v1 expression through targeting CDK13, but increased v4 expression via other targets.

Due to the high degree of homology between kinase domains of CDK12 and CDK13, it is difficult to develop selective small molecules targeting individual kinase. Thus far, only two dual inhibitors (THZ531 and SR-4835) and a CDK12 degrader (BSJ-4-116) have been discovered.<sup>25 26 43</sup> THZ531, at low concentrations (200 nM for A375; 50 nM for Hela), decreased full-length PD-L1 expression, but increased PD-L1-v4 expression, a phenotype that can be explained by enhanced IPA (figure 4D,E). However, as the THZ531 concentration increases, both full length PD-L1 and PD-L1-v4 were downregulated accordingly, suggesting that PD-L1 transcription may be inhibited at higher THZ531 concentrations like AR-A014418. The expression of STAT1 $\alpha$  and survivin was reduced by THZ531 as well (figure 4D). Furthermore, it was reported



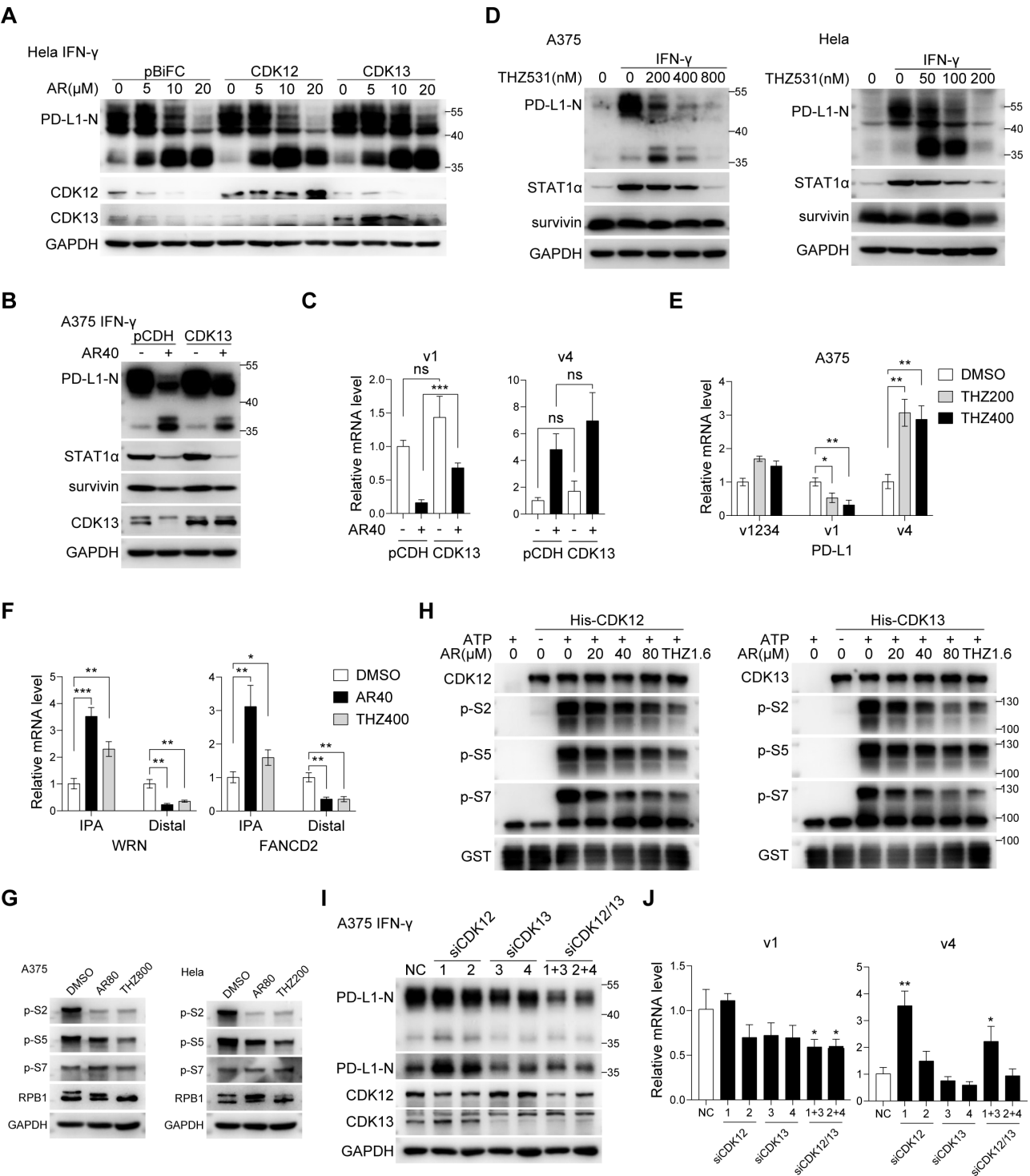


**Figure 4** AR-A014418 regulates PD-L1 expression through targeting CDK12/CDK13. (A) Western blot analysis of HeLa cells transiently transfected with the vector or pBiFC-CDK12/CDK13 followed by IFN- $\gamma$  and AR-A014418 (0, 5, 10 or 20  $\mu$ M) treatment. (B–C) Control or CDK13 overexpressing A375 stable cells were cultured with IFN- $\gamma$  and AR-A014418 (40  $\mu$ M). Cells were analyzed by western blot (B, at 24 hours) or RT-qPCR (C, 12 hours). (D) A375 and HeLa cells were treated with IFN- $\gamma$  and THZ531 at the indicated concentrations for 24 hours, then assessed by western blot. (E) A375 cells treated with IFN- $\gamma$  and THZ531 (0, 200 or 400 nM) for 12 hours were subjected to RT-qPCR experiments. (F) IPA of WRN and FANCD2 were detected by RT-qPCR in A375 cells treated with DMSO, AR-A014418 (40  $\mu$ M) or THZ531 (400 nM). (G) Western blot analysis of RPB1 CTD phosphorylation in A375 and HeLa cells treated with AR-A014418 or THZ531 at the indicated concentrations for 14 hours. (H) In vitro kinase assays of recombinant His-CDK12 and His-CDK13 using GST-tagged RPB1 CTD as substrate. Protein purification and kinase activity assays were performed as described in the ‘online supplemental methods’ section. (I–J) Western blot (I) and RT-qPCR (J) analysis of CDK12 and/or CDK13 knockdown A375 cells. In C–F, and J, the values are presented as mean  $\pm$  SD (n=3 independent experiments); \*p<0.05, \*\*p<0.01, \*\*\*p<0.001. IFN, interferon; mRNA, messenger RNA; PD-L1, programmed death ligand 1; RT-qPCR, reverse transcription-quantitative polymerase chain reaction.

that THZ531 increased IPA usage and decreased distal polyadenylation usage of DNA repair genes, including WRN and FANCD2.<sup>27</sup> AR-A014418 treatment had similar effects (figure 4F). Together, these results indicated that AR-A014418 and THZ531 may act in the same regulatory pathway.

The most well-studied substrate of CDK12/CDK13 is the CTD of RPB1 (a core subunit of Pol II complex), which contains 52 heptad repeats ( $Y_1S_2P_3T_4S_5P_6S_7$ ) in humans. Both CDK12 and CDK13 phosphorylate CTD at S2 and S5 in *in vitro* kinase assays using recombinant proteins, and THZ531 was reported to suppress phosphorylation of CTD at S2 in human Jurkat cells and Kelly E9R NB cells.<sup>23–25</sup> We first detected the changes of CTD phosphorylation in A375 and Hela cells treated with AR-A014418 or THZ531. As shown in figure 4G, the two inhibitors substantially reduced S2 and S5 phosphorylation. Incubation of GST-CTD with recombinant CDK12/cyclin K or CDK13/cyclin K in the presence of adenosine triphosphate (ATP) substantially increased its phosphorylation at S2, S5 and S7, and the phosphorylation was reversed by AR-A014418 and THZ531 (figure 4F). Thus, AR-A014418 functioned as an inhibitor of CDK12 and CDK13 kinase activity. Thermal shift assays, based on the discovery that ligand binding alters the thermostability of target proteins, were widely used to evaluate direct drug–protein interactions.<sup>44</sup> The results that AR-A014418 increased the stability of CDK12, CDK13, GSK3 $\alpha$  and GSK3 $\beta$  (online supplemental figure S5B), and THZ531 increased the stability of CDK12 and CDK13 (online supplemental figure S5C), further confirmed the direct binding of AR-A014418 to CDK12, CDK13, GSK3 $\alpha$  and GSK3 $\beta$ , and THZ531 to CDK12 and CDK13 in solution.

We next sought to determine the regulatory roles of CDK12 and CDK13 in PD-L1 expression by RNA interference. Knockdown of CDK12 increased the expression of v4, but v1 expression was not reduced, that can be attributed to low IPA proportion. Knockdown of CDK13 slightly inhibited the expression of both v1 and v4, thus CDK13 may not be involved in IPA regulation. CDK12 and CDK13 double knockdown resulted in decreased v1 and increased v4 like AR-A014418 and THZ531 treatment (figure 4I,J; Online supplemental figure S5D). Together, these results uncover that AR-A014418 may promote IPA by targeting CDK12 and repress transcription by targeting CDK13.

### AR-A014418 potentiates T-cell cytotoxicity against tumor cells

It has been well established that full-length PD-L1 on tumor cell surfaces exerts immunosuppressive effects through binding to PD-1 on activated T lymphocytes, and reducing PD-L1 levels, either genetically or pharmacologically, would substantially decrease PD-1 binding, thus enhance T-cell cytotoxicity.<sup>8,36</sup> As expected, IFN- $\gamma$  stimulation augmented PD-1 binding to A375 cells, which was effectively reversed by AR-A014418 treatment (figure 5A). Infiltrating T lymphocytes stimulate PD-L1 expression in tumor cells, acting as a negative feedback mechanism to

limit their antitumor activity. Consistent with this theory, the expression of PD-L1 (full length PD-L1 and PD-L1-v4) was upregulated rapidly and potently in A375 cells co-cultured with activated T cells (figure 5B). Both AR-A014418 and THZ531 suppressed full-length PD-L1 induction, yet increased PD-L1-v4 induction (figure 5C,D). It is puzzling that knocking out PD-L1 in A375 cells did not significantly enhance T cell-mediated tumor cell killing (data not shown). Other checkpoints, instead of PD-L1, may play a major role in A375 cells. Thus, we performed T cell-mediated killing assays by co-culturing activated T cells with MDA-MB-231 cells, in which immunosuppressive effects of PD-L1 were previously verified.<sup>8</sup> As shown in figure 5E and online supplemental figure S6A, the influence of AR-A014418 and THZ531 on PD-L1, STAT1 $\alpha$ , survivin, and 4E-BP1 expression or phosphorylation in MDA-MB-231 cells was consistent with in A375 cells. MDA-MB-231 cells were sensitive to T cell killing (only about 45% survival when co-cultured with T cells), AR-A014418 or THZ531 alone induced tumor cell death, but the combination of T cells and drug treatment almost completely abrogated MDA-MB-231 cell survival (figure 5F). These results suggested that AR-A014418 and THZ531 potentiates T-cell cytotoxicity against tumor cells.

In reality, tumor cells encounter T cells in the tumor microenvironment and PD-L1 expression has been induced before drug treatment. To investigate whether AR-A014418 can also decrease the level of full-length PD-L1 that has been stimulated by factors from T cells, MDA-MB-231 cells were preincubated with T-cell conditioned medium for more than 3 days until the mRNA and protein reached a steady-state. As shown in figure 5G and figure 5H, AR-A014418 reduced the expression of full-length PD-L1 mRNA and protein effectively. The cytotoxicity of activated T cells that have been precultured with tumor cells was enhanced by AR-A014418 as well (figure 5I).

PD-L1-v4 retains the capacity to bind PD-1, but weaker than full-length PD-L1.<sup>17</sup> Recombinant PD-L1-v4, at high concentrations, slightly inhibit T-cell activity, manifested as decreased interleukin-2 and IFN- $\gamma$  production.<sup>17,18</sup> However, secreted PD-L1-v4 from the culture supernatant of PD-L1-v4-overexpressed PC9 cells had no effect on T-cell receptor signaling of Jurkat cells, and overexpression of PD-L1-v4 on PD-L1 knockout MC38 cells did not help tumor growth *in vivo*, thus PD-L1-v4 alone may not be immunosuppressive.<sup>45</sup> Ng *et al* showed that although PD-L1-v4 had no effect on T-cell activation itself, it acted as a PD-1 antagonist, blocking the suppressive action of full-length PD-L1, and overexpression of PD-L1-v4 on MCA-38 cells significantly delayed *in vivo* tumor growth, even comparable to the extent of anti-PD-L1 blockade.<sup>41</sup> More research is needed to confirm the effects of PD-L1-v4 on antitumor immunity, suppressive, non-functional, or promoting?

To determine the influence of PD-L1-v4 on T-cell cytotoxicity against tumor cells, WT or PD-L1 knockout MDA-MB-231 cells that stably overexpress full-length PD-L1 or PD-L1-v4 were used for T-cell killing assays. The PD-1 binding ability of exogenous full-length PD-L1 was

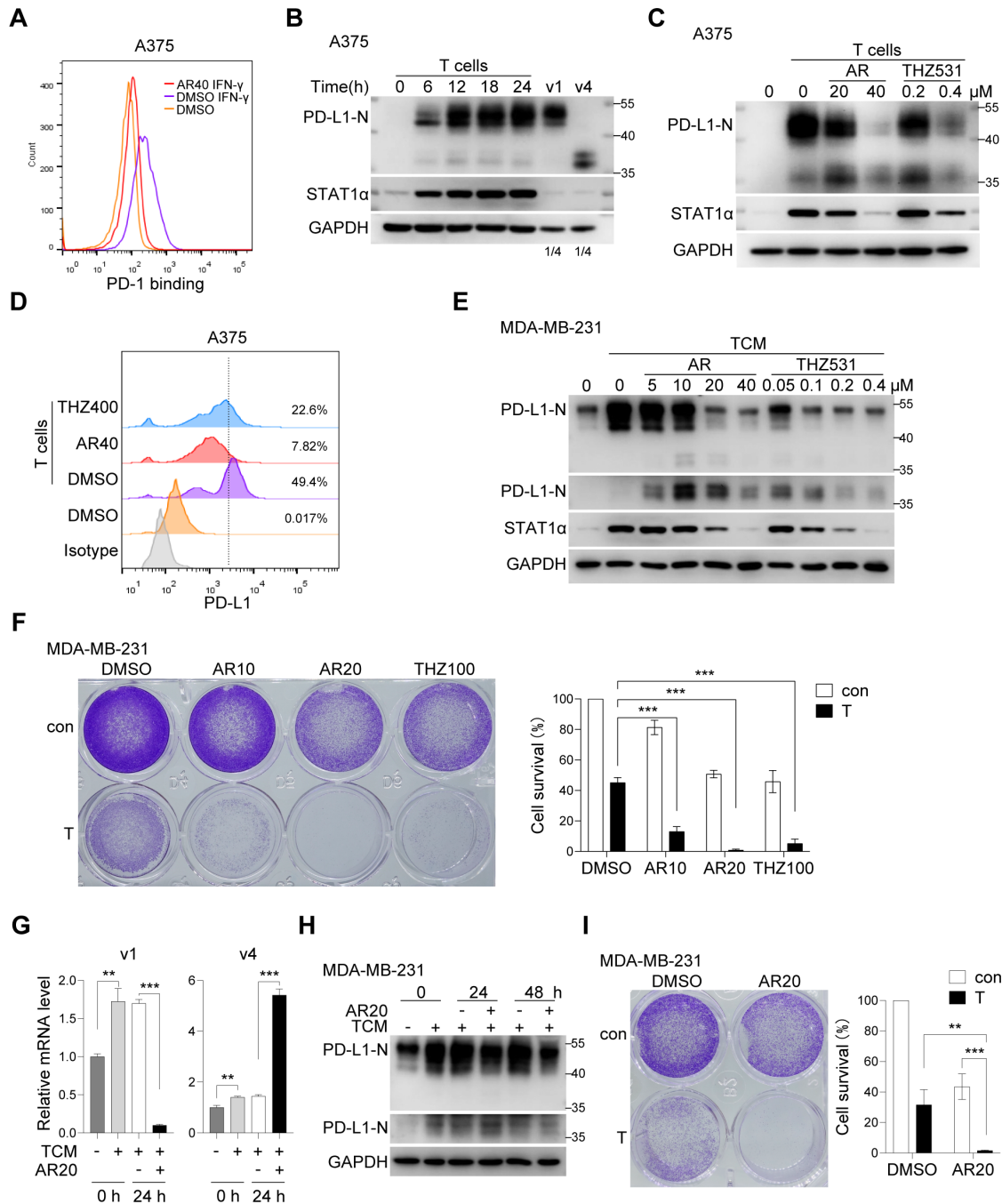


**Figure 5** AR-A014418 decreases PD-1 binding and potentiates tumor cell killing by T cells. (A) Flow cytometry quantification of PD-1 binding to A375 cells treated with IFN- $\gamma$  together with or without AR-A014418 (40  $\mu$ M) for 24 hours. (B–C) A375 cells were co-cultured with activated T cells (1:3) for the indicated time (B) or in the presence of AR-A014418 (20, 40  $\mu$ M) or THZ531 (200, 400 nM) for 24 hours (C). The living A375 cells were analyzed by western blot after removing T cells and cell debris. A375-pCDH-PD-L1-v1 (fourfold dilution) and A375-pCDH-PD-L1-v4 (fourfold dilution) were used as positive control. (D) Flow cytometry analysis of cell surface PD-L1 levels on A375 cells co-cultured with T cells. (E) Conditioned medium from activated T cells (TCM, fivefold dilution with fresh culture medium) was used to culture MDA-MB-231 cells in the presence of AR-A014418 (5, 10, 20 or 40  $\mu$ M) or THZ531 (50, 100, 200 or 400 nM). After 24 hours culture, cells were examined by western blot. (F) MDA-MB-231 cells co-cultured with activated T cells (MDA-MB-231-to-T cell ratio=1:2) for 48 hours with or without AR-A014418 (10 or 20  $\mu$ M) or THZ531 (100 nM) were subjected to crystal violet staining. Relative fold ratios of surviving cell intensities are shown on the right. (G–H) MDA-MB-231 cells were preincubated with TCM for more than 3 days. DMSO/AR-A014418 (20  $\mu$ M) were added to the culture medium at 0 hour. Samples were collected at 24 hours for RT-qPCR (G) or at 24 and 48 hours for western blot (H). (I) MDA-MB-231 cells were co-cultured with activated T cells (MDA-MB-231-to-T cell ratio=1:1.5) for 36 hours, then DMSO/AR-A014418 (20  $\mu$ M) were added to the co-culture system for another 48 hours and surviving tumor cells were subjected to crystal violet staining. The values are presented as mean $\pm$ SD (n=3 independent experiments); \*\*\*p<0.001. IFN, interferon; mRNA, messenger RNA; PD-1, programmed death 1; PD-L1, programmed death ligand 1; RT-qPCR, reverse transcription-quantitative polymerase chain reaction.



previously confirmed in A375 cells (online supplemental figure S6B). As shown in online supplemental figure S6C, overexpression of PD-L1-v4 in WT MDA-MB-231 cells slightly but not significantly reduced cell survival, suggesting that PD-L1-v4 did not obviously affect the immunosuppressive function of full-length PD-L1. Unexpectedly, overexpression of full-length PD-L1 in WT MDA-MB-231 cells failed to attenuate T cell-mediated killing, most likely because the rapidly and potently induced endogenous PD-L1 masked the effects of exogenous PD-L1. Next, we sought to evaluate the immunoregulatory functions of full-length PD-L1 and PD-L1-v4 in PD-L1 knockout MDA-MB-231 cells. Knocking out endogenous PD-L1 enhanced T-cell cytotoxicity against MDA-MB-231 cells, full-length PD-L1 rescued tumor cell survival, but PD-L1-v4 had no effect (online supplemental figure S6D).

Altogether, AR-A014418 and THZ531 enhanced T-cell cytotoxicity against tumor cells by downregulating full-length PD-L1 expression. Although PD-L1-v4 was upregulated accordingly, it had no obvious effect on T-cell immunity in the co-culture system.

## DISCUSSION

Immune checkpoint inhibitors (ICIs) aim to restore the antitumor immunity by increasing the infiltration and activity of CTLs and natural killer cells. Cytokines released by these cells, especially IFN- $\gamma$ , induce significant upregulation of PD-L1 on tumor cells. High PD-L1 protein level may discount the effects of anti-PD-L1 antibodies, or limit the function of CTLs. Thus, small-molecule inhibitors, decreasing PD-L1 expression, could synergistically enhance the antitumor activity of various ICIs.<sup>3,7–9</sup> Several different forms of extracellular PD-L1, such as exosomal PD-L1 or soluble splice variants, have been identified to directly suppress the cytotoxicity of CTLs or work as ‘decoys’ for anti-PD-L1 therapies.<sup>46–48</sup> Besides cell membrane or extracellular space localization, PD-L1 can also translocate into the nucleus of numerous cancer cells, where it will not be recognized by antibodies.<sup>8,49</sup> Interfering PD-L1 expression, extracellular or nuclear localization, and activity with small-molecule inhibitors would open a new avenue for tumor immunotherapy, and cannot be covered by antibody drugs.

Here, we found that AR-A014418 decreased IFN- $\gamma$  induced full-length PD-L1 expression and potentiated T cell-mediated tumor cell killing. To determine whether AR-A014418 could activate antitumor immunity in vivo, subcutaneous xenograft tumor models (B16F10 melanoma, CT26 colon cancer) and lung metastases model (B16F10 melanoma) were used. The maximum solubility of AR-A014418 in 10% DMSO+40% PEG300+5% Tween-80+45% saline was 1 mg/mL for intraperitoneal injection and in 5% DMSO+5% Tween-80+90% saline was 0.5 mg/mL for intravenous injection. Unexpectedly, AR-A014418 treatment by both intraperitoneal (20 mg/kg) or intravenous (10 mg/kg) injection did not delay tumor growth (data not shown). The phosphorylation of GSK3 $\alpha/\beta$  in

tumor tissues was not inhibited even that needs a lower AR-A014418 concentration. That is to say, AR-A014418 did not reach its therapeutic concentrations in tumor tissues, partly because of the very low solubility. It is necessary to increase the solubility and bioavailability of AR-A014418 by chemical modifications.

Despite inhibiting CDK12 and CDK13 have been well documented to disable the expression of full-length products of long genes with multiple PA-sites by triggering IPA.<sup>24–26,28</sup> For a specific gene, IPA alone may not be enough to profoundly block full-length transcription. In the present work, we tentatively concluded that the roles of CDK12 and CDK13 in PD-L1 expression seem different, CDK12 limits the IPA at intron 4 but CDK13 regulates the transcription of PD-L1, AR-A014418 targeting CDK12 and CDK13 to enhance IPA and repress transcription, respectively. To verify this conclusion, Pol II density along the PD-L1 gene with or without AR-A014418 treatment needs to be investigated in further study.

**Contributors** GZ and BL conceived the project, designed and carried out the experiments, and wrote the manuscript. XZ and JC revised and validated the manuscript. ML and YL helped to construct several recombinant plasmids. FG is responsible for the overall content as the guarantor.

**Funding** This work was supported by the National Natural Science Foundation of China (No.81672310 and 81472610).

**Competing interests** None declared.

**Patient consent for publication** Not applicable.

**Ethics approval** Not applicable.

**Provenance and peer review** Not commissioned; externally peer reviewed.

**Data availability statement** All data relevant to the study are included in the article or uploaded as supplementary information.

**Supplemental material** This content has been supplied by the author(s). It has not been vetted by BMJ Publishing Group Limited (BMJ) and may not have been peer-reviewed. Any opinions or recommendations discussed are solely those of the author(s) and are not endorsed by BMJ. BMJ disclaims all liability and responsibility arising from any reliance placed on the content. Where the content includes any translated material, BMJ does not warrant the accuracy and reliability of the translations (including but not limited to local regulations, clinical guidelines, terminology, drug names and drug dosages), and is not responsible for any error and/or omissions arising from translation and adaptation or otherwise.

**Open access** This is an open access article distributed in accordance with the Creative Commons Attribution Non Commercial (CC BY-NC 4.0) license, which permits others to distribute, remix, adapt, build upon this work non-commercially, and license their derivative works on different terms, provided the original work is properly cited, appropriate credit is given, any changes made indicated, and the use is non-commercial. See <http://creativecommons.org/licenses/by-nc/4.0/>.

## ORCID iD

Ganggang Zhang <http://orcid.org/0000-0001-9490-9925>

## REFERENCES

- 1 Zou W, Chen L. Inhibitory b7-family molecules in the tumour microenvironment. *Nat Rev Immunol* 2008;8:467–77.
- 2 McDermott DF, Lee J-L, Ziobro M, et al. Open-Label, single-arm, phase II study of pembrolizumab monotherapy as first-line therapy in patients with advanced non-clear cell renal cell carcinoma. *J Clin Oncol* 2021;39:1029–39.
- 3 Lu C, Paschall AV, Shi H, et al. The ml1-h3k4me3 axis-mediated pd-l1 expression and pancreatic cancer immune evasion. *J Natl Cancer Inst* 2017;109:djw283.
- 4 Du L, Lee J-H, Jiang H, et al. B-Catenin induces transcriptional expression of PD-L1 to promote glioblastoma immune evasion. *J Exp Med* 2020;217:11.

- 5 Coelho MA, de Carné Trécesson S, Rana S, *et al.* Oncogenic Ras signaling promotes tumor immunoresistance by stabilizing PD-L1 mRNA. *Immunity* 2017;47:1083–1099.
- 6 Xu Y, Poggio M, Jin HY, *et al.* Translation control of the immune checkpoint in cancer and its therapeutic targeting. *Nat Med* 2019;25:301–11.
- 7 Li C-W, Lim S-O, Xia W, *et al.* Glycosylation and stabilization of programmed death ligand-1 suppresses t-cell activity. *Nat Commun* 2016;7:12632:12632..
- 8 Cha J-H, Yang W-H, Xia W, *et al.* Metformin promotes antitumor immunity via endoplasmic-reticulum-associated degradation of pd-l1. *Mol Cell* 2018;71:S1097-2765(18)30599-9:606–620..
- 9 Wu Y, Zhang C, Liu X, *et al.* ARIH1 signaling promotes anti-tumor immunity by targeting PD-L1 for proteasomal degradation. *Nat Commun* 2021;12.
- 10 Wang H, Yao H, Li C, *et al.* Hip1R targets PD-L1 to lysosomal degradation to alter T cell-mediated cytotoxicity. *Nat Chem Biol* 2019;15:42–50.
- 11 Jiao S, Xia W, Yamaguchi H, *et al.* Parp inhibitor upregulates PD-L1 expression and enhances cancer-associated immunosuppression. *Clin Cancer Res* 2017;23:3711–20.
- 12 Li H, Li C-W, Li X, *et al.* Met inhibitors promote liver tumor evasion of the immune response by stabilizing PDL1. *Gastroenterology* 2019;156:S0016-5085(19)30349-X:1849–1861..
- 13 Dong H, Zhu G, Tamada K, *et al.* B7-H1, a third member of the B7 family, co-stimulates T-cell proliferation and interleukin-10 secretion. *Nat Med* 1999;5:1365–9.
- 14 Freeman GJ, Long AJ, Iwai Y, *et al.* Engagement of the PD-1 immunoinhibitory receptor by a novel B7 family member leads to negative regulation of lymphocyte activation. *J Exp Med* 2000;192:1027–34.
- 15 He X, Xu L, Liu Y. Identification of a novel splice variant of human PD-L1 mRNA encoding an isoform-lacking igv-like domain. *Acta Pharmacol Sin* 2005;26:462–8.
- 16 Qu S, Jiao Z, Lu G, *et al.* Pd-L1 lncRNA splice isoform promotes lung adenocarcinoma progression via enhancing c-myc activity. *Genome Biol* 2021;22:104.
- 17 Hassounah NB, Malladi VS, Huang Y, *et al.* Identification and characterization of an alternative cancer-derived PD-L1 splice variant. *Cancer Immunol Immunother* 2019;68:407–20.
- 18 Mahoney KM, Shukla SA, Patsoukis N, *et al.* A secreted PD-L1 splice variant that covalently dimerizes and mediates immunosuppression. *Cancer Immunol Immunother* 2019;68:421–32.
- 19 Hoque M, Ji Z, Zheng D, *et al.* Analysis of alternative cleavage and polyadenylation by 3' region extraction and deep sequencing. *Nat Methods* 2013;10:133–9.
- 20 Yuan F, Hankey W, Wagner EJ, *et al.* Alternative polyadenylation of mRNA and its role in cancer. *Genes Dis* 2021;8:61–72.
- 21 Blazek D, Kohoutek J, Bartholomeeusen K, *et al.* The cyclin K/cdk12 complex maintains genomic stability via regulation of expression of DNA damage response genes. *Genes Dev* 2011;25:2158–72.
- 22 Liang K, Gao X, Gilmore JM, *et al.* Characterization of human cyclin-dependent kinase 12 (CDK12) and CDK13 complexes in C-terminal domain phosphorylation, gene transcription, and RNA processing. *Mol Cell Biol* 2015;35:928–38.
- 23 Greifenberg AK, Hönig D, Pilarova K, *et al.* Structural and functional analysis of the cdk13/cyclin K complex. *Cell Reports* 2016;14:320–31.
- 24 Krajewska M, Dries R, Grassetti AV, *et al.* Cdk12 loss in cancer cells affects DNA damage response genes through premature cleavage and polyadenylation. *Nat Commun* 2019;10:1757.
- 25 Zhang T, Kwiatkowski N, Olson CM, *et al.* Covalent targeting of remote cysteine residues to develop CDK12 and CDK13 inhibitors. *Nat Chem Biol* 2016;12:876–84.
- 26 Quereda V, Bayle S, Vena F, *et al.* Therapeutic targeting of cdk12/cdk13 in triple-negative breast cancer. *Cancer Cell* 2019;36:S1535-6108(19)30424-6:545–558..
- 27 Dubbury SJ, Boutz PL, Sharp PA. CDK12 regulates dna repair genes by suppressing intronic polyadenylation. *Nature* 2018;564:141–5.
- 28 Fan Z, Devlin JR, Hogg SJ, *et al.* Cdk13 cooperates with CDK12 to control global RNA polymerase II processivity. *Sci Adv* 2020;6:18.
- 29 Bhat R, Xue Y, Berg S, *et al.* Structural insights and biological effects of glycogen synthase kinase 3-specific inhibitor AR-A014418. *J Biol Chem* 2003;278:45937–45.
- 30 Martelli AM, Paganelli F, Evangelisti C, *et al.* Pathobiology and therapeutic relevance of GSK-3 in chronic hematological malignancies. *Cells* 2022;11:1812.
- 31 Abiko K, Matsumura N, Hamanishi J, *et al.* Ifn- $\gamma$  from lymphocytes induces PD-L1 expression and promotes progression of ovarian cancer. *Br J Cancer* 2015;112:1501–9.
- 32 Hughes K, Nikolakaki E, Plyte SE, *et al.* Modulation of the glycogen synthase kinase-3 family by tyrosine phosphorylation. *EMBO J* 1993;12:803–8.
- 33 Carter YM, Kunnimalaiyaan S, Chen H, *et al.* Specific glycogen synthase kinase-3 inhibition reduces neuroendocrine markers and suppresses neuroblastoma cell growth. *Cancer Biol Ther* 2014;15:510–5.
- 34 Shin S, Wolgamott L, Tcherkezian J, *et al.* Glycogen synthase kinase-3 $\beta$  positively regulates protein synthesis and cell proliferation through the regulation of translation initiation factor 4E-binding protein 1. *Oncogene* 2014;33:1690–9.
- 35 Garcia-Diaz A, Shin DS, Moreno BH, *et al.* Interferon receptor signaling pathways regulating PD-L1 and PD-L2 expression. *Cell Rep* 2019;29:S2211-1247(19)31636-5:3766..
- 36 Cerezo M, Guemiri R, Druillennec S, *et al.* Translational control of tumor immune escape via the eif4f-stat1-pd-l1 axis in melanoma. *Nat Med* 2018;24:1877–86.
- 37 Biswas B, Guemiri R, Cadix M, *et al.* Differential effects on the translation of immune-related alternatively polyadenylated mRNAs in melanoma and t cells by eif4a inhibition. *Cancers (Basel)* 2022;14:1177.
- 38 Orme JJ, Jazieh KA, Xie T, *et al.* ADAM10 and adam17 cleave pd-l1 to mediate pd-(l)1 inhibitor resistance. *Oncimmunology* 2020;9:..1744980.
- 39 Romero Y, Wise R, Zolkiewska A. Proteolytic processing of pd-l1 by adam proteases in breast cancer cells. *Cancer Immunol Immunother* 2020;69:43–55.
- 40 Sanz E, Yang L, Su T, *et al.* Cell-type-specific isolation of ribosome-associated mRNA from complex tissues. *Proc Natl Acad Sci U S A* 2009;106:13939–44.
- 41 Ng KW, Attig J, Young GR, *et al.* Soluble PD-L1 generated by endogenous retroelement exaptation is a receptor antagonist. *Elife* 2019;8:e50256.
- 42 Parua PK, Fisher RP. Dissecting the pol II transcription cycle and derailing cancer with CDK inhibitors. *Nat Chem Biol* 2020;16:716–24.
- 43 Jiang B, Gao Y, Che J, *et al.* Discovery and resistance mechanism of a selective CDK12 degrader. *Nat Chem Biol* 2021;17:675–83.
- 44 Dziekan JM, Wirjanata G, Dai L, *et al.* Cellular thermal shift assay for the identification of drug-target interactions in the Plasmodium falciparum proteome. *Nat Protoc* 2020;15:1881–921.
- 45 Sagawa R, Sakata S, Gong B, *et al.* Soluble PD-L1 works as a decoy in lung cancer immunotherapy via alternative polyadenylation. *JCI Insight* 2022;7.
- 46 Chen G, Huang AC, Zhang W, *et al.* Exosomal PD-L1 contributes to immunosuppression and is associated with anti-PD-1 response. *Nature* 2018;560:382–6.
- 47 Poggio M, Hu T, Pai C-C, *et al.* Suppression of exosomal PD-L1 induces systemic anti-tumor immunity and memory. *Cell* 2019;177:S0092-8674(19)30165-5:414–427..
- 48 Gong B, Kiyotani K, Sakata S, *et al.* Secreted PD-L1 variants mediate resistance to PD-L1 blockade therapy in non-small cell lung cancer. *J Exp Med* 2019;216:982–1000.
- 49 Gao Y, Nihira NT, Bu X, *et al.* Acetylation-Dependent regulation of PD-L1 nuclear translocation dictates the efficacy of anti-PD-1 immunotherapy. *Nat Cell Biol* 2020;22:1064–75.